Biochemical and Biophysical Research Communications 462 (2015) 14–20

Contents lists available at ScienceDirect

Biochemical and Biophysical Research Communications

journal homepage: www.elsevier.com/locate/ybbrc

Simultaneous ternary extension of DNA catalyzed by a trimeric replicase assembled *in vivo*

Alejandro Montón Silva [a], Fabio Lapenta [a], Alessandra Stefan [a, b], Fabrizio Dal Piaz [c], Alessandro Ceccarelli [a], Alessandro Perrone [a], Alejandro Hochkoeppler [a, b, *]

[a] Department of Pharmacy and Biotechnology, University of Bologna, Viale Risorgimento 4, 40136 Bologna, Italy
[b] CSGI, University of Firenze, Via della Lastruccia 3, 50019 Sesto Fiorentino, FI, Italy
[c] Department of Pharmacy, University of Salerno, Via Giovanni Paolo II 132, 84084 Fisciano, SA, Italy

ARTICLE INFO

Article history:
Received 31 March 2015
Available online 25 April 2015

Keywords:
Trimeric DNA Polymerase
E. coli
DNA Polymerase III
$\tau_3\alpha_3\varepsilon_3\theta_3$ complex
Triple DNA extension

ABSTRACT

According to current models, dimeric DNA Polymerases coordinate the replication of DNA leading and lagging strands. However, it was recently shown that trimeric DNA Polymerases, assembled *in vitro*, replicate the lagging strand more efficiently than dimeric replicases. Here we show that the τ, α, ε, and θ subunits of *Escherichia coli* DNA Polymerase III can be assembled *in vivo*, yielding the trimeric $\tau_3\alpha_3\varepsilon_3\theta_3$ complex. Further, we propose a molecular model of this complex, whose catalytic action was investigated using model DNA substrates. Our observations indicate that trimeric DNA replicases reduce the gap between leading and lagging strand synthesis.

1. Introduction

In *Escherichia coli*, DNA Polymerase III (DNA Pol-III) is competent in genome replication, and is considered an asymmetric dimer, containing 10 different subunits, i.e. α, ε, θ, τ, γ, ψ, χ, δ, δ′, and β [1]. The α, ε, and θ subunits are tightly associated into a catalytic core, with α providing the 5′-3′ Pol activity [2], and ε the 3′-5′ exonuclease (proofreading) activity [3]. The θ subunit increases the stability of ε [4], the bridging subunit of the core interacting with both α and θ [5]. The τ subunit features ATPase activity [6], self-interacts [7], and contacts α [8], therefore assembling independent catalytic cores. Interestingly, the γ subunit is coded by the same gene (*dnaX*) yielding τ. A frameshift in translation of the *dnaX* message is indeed responsible for early termination, producing a C-ter truncated form of τ, i.e. the γ subunit [9]. Moreover, it was demonstrated that using a mutant form of *dnaX*, devoid of the frameshift motif, only the τ subunit is expressed [10]. Due to the deficiency of the τ C-ter region, γ is not competent in binding α. However, two independent catalytic cores can associate via the DnaX complex, composed of the τ, γ, ψ, χ, δ, and δ′ subunits, assembled according to $\tau_2\gamma_1\psi_1\chi_1\delta_1\delta'_1$ stoichiometry. This dimeric replicase, denominated Pol-III*, can withstand the simultaneous synthesis of leading and lagging DNA strands [11]. In addition, high processivity is conferred to *E. coli* Pol III* by the β subunit, acting as a clamp on DNA [12] and interacting with α [13]. Recently, a trimeric replicase containing 3 τ subunits and 3 catalytic cores was assembled *in vitro*, and it was shown that the 3 active sites of this replicase are able to exert their Pol function simultaneously, and outperform their dimeric counterparts in lagging strand replication [14–17]. Here we report on the trimeric complex $\tau_3\alpha_3\varepsilon_3\theta_3$, assembled *in vivo*. In particular, the action of this trimeric replicase at the expense of double- and single-primed DNAs is presented here, along with a molecular model which relies on α-α interactions detected by mass spectroscopy.

2. Materials and methods

2.1. Bacterial cultures and media

E. coli TOP10 (obtained from Invitrogen, Carlsbad, USA), was transformed with the plasmid pBAD-α [18], and was eventually co-transformed with pGOOD-ε-θ [19] or with pGOOD-$\tau_{\gamma less}$-ε-θ. The transformants were grown at 30 °C for 15 h, using LB medium supplemented with the appropriate antibiotics. The α subunit, the catalytic core, or the $\tau_3\alpha_3\varepsilon_3\theta_3$ complex were overexpressed for 2.5 h with arabinose alone or arabinose and IPTG (1 mM each).

* Corresponding author. Department of Pharmacy and Biotechnology, University of Bologna, Viale Risorgimento 4, 40136 Bologna, Italy. Fax: +39 051 2093673.
E-mail address: a.hochkoeppler@unibo.it (A. Hochkoeppler).

http://dx.doi.org/10.1016/j.bbrc.2015.04.067
0006-291X/

2.2. Construction of pGOOD-$\tau_{\gamma less}$-ε-θ

The *dna*X-γless gene was synthesized by Entelechon GmbH (Bad Abbach, Germany). To obtain overexpression of the τ subunit only, the sequence responsible for the translational frameshift yielding γ subunit was mutated [10], i.e. the wild type codons 429-431 were changed to AAG-AAA-AGC. The synthetic *dna*X-γless gene was then inserted into the pGOOD plasmid, using the *NcoI* and *PstI* sites, yielding pGOOD-$\tau_{\gamma less}$. The insert coding for ε and θ subunits was then amplified from the pGOOD-ε-θ plasmid [19]. To this aim, the plasmid was linearized with *AlwNI* restriction enzyme and subjected to PCR using 5′GCTGGAGGTACCAGGAGGTGAGCTAATGGG CACTGCAATTACACGCCAGA3′ as forward and 5′GAGCTGGAATTCTT ATTTAAGTTTGGGCTCGTAAGGT3′ as reverse primer, respectively. The amplified fragment was digested with *KpnI* and *EcoRI* enzymes, and finally inserted into the pGOOD-$\tau_{\gamma less}$ vector, previously treated with the same restriction endonucleases.

2.3. Protein purification

Soluble protein extracts were loaded onto a 50 mL Q-Sepharose FF column (1.6 × 25 cm, GE Healthcare, Piscataway, USA) equilibrated with buffer A (50 mM Tris–HCl pH 8, 50 mM NaCl, 1 mM EDTA, 2.5 mM DTT). The column was then washed with 5 column volumes of buffer A, and elution was performed applying a linear NaCl gradient (50–600 mM). The best fractions, according to SDS-PAGE analysis, were pooled, diluted with buffer B (50 mM Tris–HCl pH 8, 50 mM NaCl, 1 mM EDTA, 2.5 mM DTT, 20% glycerol), concentrated, and loaded onto a 30 mL CibacronBlue 3G column (GE Healthcare, 1.6 × 15 cm), equilibrated with buffer B. After loading the sample (at 0.5 mL/min), the column was washed with 5 column volumes of equilibration buffer. Elution was performed by a two-step NaCl gradient (150 mM and 1 M NaCl) in equilibration buffer, at 2 mL/min. The peak eluted at 1 M NaCl was collected, reconditioned to 50 mM NaCl in buffer B, and then loaded onto a 5 mL HiTrap Heparin HP column (GE Healthcare), equilibrated with buffer B. After loading the sample, the column was washed, and elution was obtained with a 50 mL linear gradient of NaCl (50–300 mM in buffer B). Fractions (0.9 mL) were collected and analyzed by SDS-PAGE. The best fractions were pooled, conditioned to 50 mM NaCl in buffer B, concentrated, and finally loaded onto a 1 mL ResourceQ pre-packed column (GE Healthcare). The best fractions (0.2 mL) were pooled to yield purified α subunit or αεθ catalytic core.

When the $\tau_3\alpha_3\varepsilon_3\theta_3$ was purified, the best fractions eluted from the HiTrap Heparin column were concentrated to 1 mL and loaded onto a Sephacryl S-300 column (GE Healthcare, 1.6 × 62 cm), equilibrated with 50 mM Tris–HCl pH 8, 150 mM NaCl, 1 mM EDTA, 2.5 mM DTT, 20% glycerol (v/v). Elution was performed at 0.6 mL/min, and fractions of 0.9 mL were collected. The column was calibrated with HMW Gel Filtration Calibration kit (GE Healthcare). Protein concentration was determined according to Bradford [20].

2.4. Mass spectrometry

Cross-linking of subunits of the $\tau_3\alpha_3\varepsilon_3\theta_3$ complex was obtained by incubation, for 1 h at room temperature, with 50 μM bis(sulfosuccinimidyl)suberate (BS3) in phosphate-buffered saline (pH 7.2). The cross-linking reaction was stopped by the addition of 100 mM Tris-HCl buffer, pH 7.9. Mass Spectrometry was performed as previously described [21].

ESI-MS measurements of the native $\tau_3\alpha_3\varepsilon_3\theta_3$ complex were performed in positive ion mode, using a modified electrospray ionization quadrupole-time-of-flight instrument (Waters) equipped with a Z-spray nano-spray source. The pressure in the first vacuum stages of the mass spectrometer was increased, in order to cool the ions, leading to a higher stability *in vacuo* of ions from large complexes [22]. To this aim, pressure conditions were raised to 10 mbar and capillary and cone voltages were set to 1750 and 125 V, respectively. Analogously, the collision cell gas pressure and the collision energy were also optimized.

All spectra were mass calibrated using an aqueous solution of caesium iodide (50 mg/mL). Mass spectra were acquired in the m/z range 2000–8000 and averaged, smoothed and centered, using the software program MassLynx 4.0 (Waters). The molecular mass of the $\tau_3\alpha_3\varepsilon_3\theta_3$ complex was obtained using the MassLynx function MaxEnt.

2.5. Steady-state activity assays

For steady-state kinetic experiments, a Perkin–Elmer λ19 spectrophotometer was used. DNA Polymerase and ATPase activities were assayed by detecting the pyrophosphate and phosphate released, respectively [23]. Steady-state 3′-5′ exonuclease activity of ε subunit was determined according to Hamdan et al. [24], using 5′-*p*-nitrophenyl ester of thymidine monophosphate (pNP-TMP) as substrate. Reaction velocities were calculated using 12,600 and 12,950 M^{-1} cm^{-1} as the molar extinction coefficients for uric acid [23] at 293 and p-nitrophenolate [24] at 420 nm, respectively.

DNA Polymerase activity was assayed in the presence of 100 mM Tris-HCl (pH 8), 5 mM $MgCl_2$, 0.25 mM inosine, 1 μM DNA, and 10, 50 and 500 mU/mL of inorganic pyrophosphatase (PPase), purine nucleoside phosphorylase (PNPase), and xanthine oxidase (XOD), respectively. Reactions were started by the addition of 100 μM dNTP and monitored at 293 nm.

ATPase activity of τ subunit was assayed according to Tsuchihashi and Kornberg [6]. Reaction mixtures contained 100 mM Tris–HCl, 5 mM $MgCl_2$, 0.25 mM inosine, 1 μM ssDNA (sequence 5′AAAAAAAAGCGCGCGC3′). The inorganic phosphate released from ATP was detected using PNPase and XOD. Reactions were started by the addition of 0.4 mM ATP, and monitored at 293 nm.

To determine 3′-5′ exonuclease activity, pNP-TMP was used as substrate. Assay mixtures contained 50 mM Tris-HCl (pH 8), 150 mM NaCl, 1 mM $MnCl_2$, and 1 mM DTT. Reactions were started with 3 mM pNP-TMP, and monitored at 420 nm.

2.6. Single-turnover activity assays

DNA Polymerase activity was assayed using a stirred Hellma quartz cuvette (model 119-004-10-40) and a V-550 Jasco spectrophotometer. Assay and detection conditions were the same as for the steady-state determinations, except for substrate and enzyme concentrations, both at 0.2 μM. In addition, to ensure minimization of the lag time, PPase, PNPase, and XOD were used at 50, 500, and 500 mU/mL, respectively. Reactions were started by the addition of DNAs.

3. Results and discussion

To assess whether a trimeric replicase can be assembled *in vivo*, and to further test the τ/core stoichiometry, we co-expressed in *E. coli* the α, ε, and θ subunits, along with a *dnaX* variant unable to produce γ. With this aim, we cloned into the pBAD plasmid the *dnaE* gene (coding for α), and into the pGOOD vector [19] the *dnaX*-γless, *dnaQ,* and *holE* genes (coding for τ, ε, and θ, subunits, respectively). *E. coli* was co-transformed with these two plasmids and the overexpression of α, τ, ε, and θ was triggered by the addition of arabinose and isopropyl-thio-β-D-galactopyranoside (IPTG) to the growth medium. As a first test, we extracted soluble proteins from overexpressing cells, and we immediately loaded the protein

extract onto a Sephacryl S-300 column. Each collected fraction was then assayed for DNA Polymerase, 3′-5′ exonuclease, and ATPase activities. Surprisingly, the major and most sharp peaks of these 3 activities overlapped, and were detected at fractions containing proteins featuring molecular masses compatible with a $\tau_3\alpha_3\varepsilon_3\theta_3$ complex (Supplementary Fig. 1). On the contrary, no sharp activity peaks were observed at elution volumes corresponding to a dimeric complex (Supplementary Fig. 1). We then attempted the purification of the $\tau_3\alpha_3\varepsilon_3\theta_3$ complex by means of standard chromatographic techniques. Unexpectedly, no dimeric replicase ($\tau_2\alpha_2\varepsilon_2\theta_2$) was detected, while trimeric Polymerase ($\tau_3\alpha_3\varepsilon_3\theta_3$) was readily purified (Fig. 1A–C), along with an excess of $\alpha\varepsilon\theta$ catalytic core (Fig. 1A–C). The oligomerization state of the purified replicase was further ascertained by ESI mass spectroscopy. To this aim, a solution of the native enzyme in 25 mM ammonium acetate buffer (pH 6.5) was used. Under these conditions, we detected a major peak corresponding to a molecular mass equal to 708050 Da (Fig. 1D), in good agreement with the expected value for the $\tau_3\alpha_3\varepsilon_3\theta_3$ complex, i.e. 710238 Da. Further, to identify interactions between subunits, the trimeric complex was subjected to cross-linking (Fig. 1E), using bis(sulfosuccinimidyl)suberate (BS3). Mass spectra of the cross-linked trimeric Polymerase revealed α-ε, ε-θ, τ-τ, and α-α contacts (Supplementary Tables 1–4). The detected α-ε and ε-θ contacts confirm previously described interactions between α N-ter and ε C-ter [25], and between ε N-ter and θ [26]. Remarkably, the observed α-α interaction (engaging Lys1037 or Lys1044) resides in the C-ter region, mapping into a portion of α which is most likely disordered. Crystals of α were indeed obtained using a truncated form of α, lacking the residues 918-1169 [27].

DNA Polymerase activity was then assayed using the trimeric replicase, and the observed activity was compared to that of purified α subunit. To this aim, we used as substrate a 40mer DNA template strand paired to a single pentadecameric primer (Fig. 2A). The template and the primer were chosen to produce, once annealed, a 25mer PolydA overhang, and dTTP was used as the single dNTP substrate (Fig. 2A). Under these conditions, the 3 α subunits of $\tau_3\alpha_3\varepsilon_3\theta_3$ were found to exert their function simultaneously (Fig. 2B and D). The k_{cat} was indeed equal to 1.89 ± 0.15 and 2.59 ± 0.26 s^{-1} for α subunit and $\tau_3\alpha_3\varepsilon_3\theta_3$, respectively, suggesting a slight increase of activity in the trimeric complex. Similar observations were obtained when the 3′-5′ exonuclease activity of the trimeric replicase was assayed with the *p*-nitrophenyl ester of thymidine 5′-monophosphate (pNP-TMP). In this case, the k_{cat} values were 9.66 ± 0.36 and 8.50 ± 0.29 s^{-1} for the catalytic core and the trimeric replicase, respectively (Fig. 2C and E).

To model the replication of leading and lagging strands, we designed a set of DNAs to be used in single-turnover assays with the trimeric replicase. In particular, we devised three different double-primed DNAs (100mer, 75mer, 50mer, Fig. 2A), whose elongation requires dTTP and dATP for the extension near the 3′ (head) and the 5′ (tail) end of the template, respectively (Fig. 2A). To test how the inter-primer distance affects the simultaneous replication of template head and tail, these different DNAs contain primers 15, 40, or 65 nucleotides apart (Fig. 2A). In addition, we selected a single-primed DNA (25mer), the elongation of which depends on dGTP (Fig. 2A). Our rationale was to use the double-primed DNA as a model of lagging strand, with the single-primed DNA mimicking the leading strand (Fig. 3A). First, we performed steady-state assays using α subunit and a single substrate, i.e. 100mer, 75mer, 50mer or 25mer DNA. Under these conditions, the highest DNA Polymerase activity was observed in the presence of the 25mer DNA (Supplementary Figs 2–3). Moreover, when the double-primed

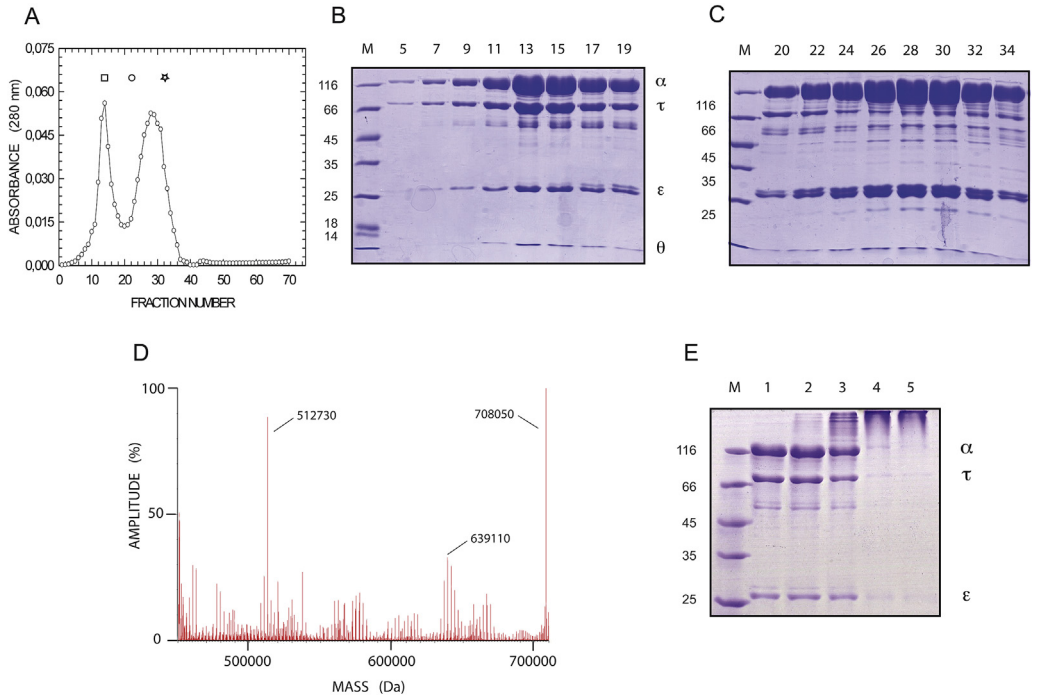

Fig. 1. Purification of the $\tau_3\alpha_3\varepsilon_3\theta_3$ complex. **A)** Gel filtration (Sephacryl S-300 column) of the trimeric replicase, previously subjected to anion-exchange and affinity chromatography. The square, circle, and star indicate the elution volume of the molecular mass markers thyroglobulin (669 kDa), ferritin (440 kDa), and catalase (232 kDa). The theoretical molecular masses of $\tau_3\alpha_3\varepsilon_3\theta_3$ and $\alpha\varepsilon\theta$ complexes are equal to 710 and 166 kDa, respectively. **B**, **C)** SDS-PAGE of fractions eluted from the Sephacryl S-300 column (the fraction numbers are indicated at the top; M: molecular mass markers). The position of α, τ, ε, and θ subunits are indicated at the right side of Fig. 1B. **D)** ESI mass spectrum of native $\tau_3\alpha_3\varepsilon_3\theta_3$ complex. The molecular masses of major peaks are indicated in Daltons. **E)** SDS-PAGE of purified $\tau_3\alpha_3\varepsilon_3\theta_3$ complex subjected or not to cross-linking with BS3. The trimeric replicase (350 nM) was incubated with 5, 50, 500, or 1000 μM BS3 in PBS (lanes 2-5, respectively), for 1 h at room temperature. Reactions were blocked by the addition of 100 mM Tris–HCl, pH 7.9. Lane 1 was loaded with an aliquot of untreated $\tau_3\alpha_3\varepsilon_3\theta_3$ complex.

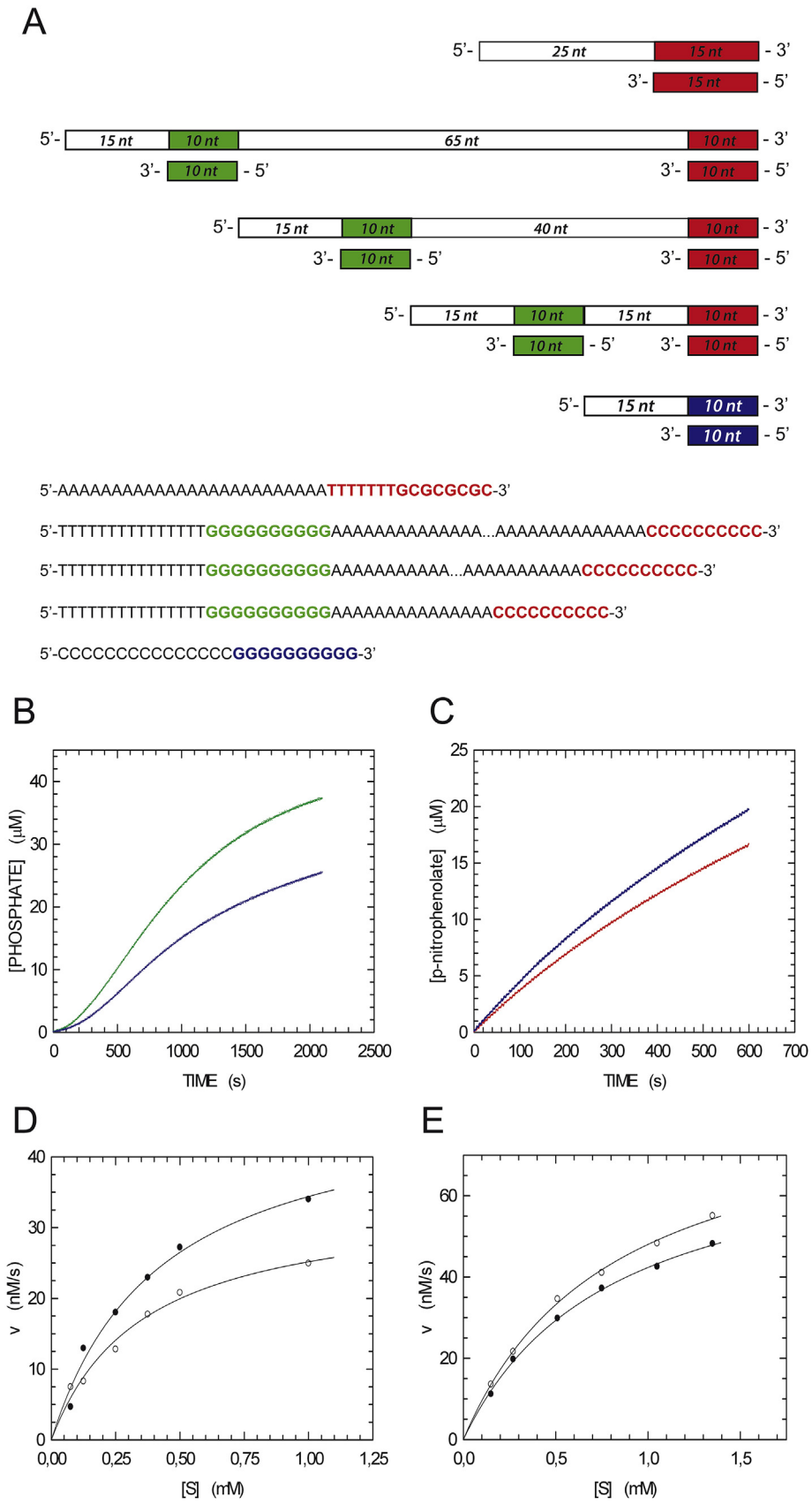

Fig. 2. Scheme of the DNAs used in the present work, and steady-state assays of DNA Polymerase and 3′-5′ exonuclease activity. **A)** Cartoon and template strand sequences of the different DNAs designed for steady-state and single-turnover assays. **B)** Steady-state assay of DNA Polymerase activity of 17.4 nM α subunit (green dots) and 3.2 nM $\tau_3\alpha_3\varepsilon_3\theta_3$ complex (blue dots), in the presence of 1 μM 40mer DNA (Fig. 2A) and 100 μM dTTP. **C)** Steady-state assay of 3′-5′ exonuclease activity of 5.3 nM αεθ catalytic core (red dots) and 1.8 nM $\tau_3\alpha_3\varepsilon_3\theta_3$ complex (blue dots), in the presence of 3 mM *p*-nitrophenyl ester of 5'-thymidine monophosphate (pNP-TMP). **D**, **E)** Initial velocities of DNA Polymerase (Panel D) and 3′-5′ exonuclease (Panel E) reactions as a function of DNA and pNP-TMP concentration, respectively. Reactions were catalyzed by 18 nM α subunit (empty circles, Panel D), 6.3 nM or 3.1 nM $\tau_3\alpha_3\varepsilon_3\theta_3$ complex (filled circles, Panels D and E, respectively), and 9 nM αεθ catalytic core (empty circles, Panel E). The continuous lines represent best fits to the Michaelis-Menten equation. (For interpretation of the references to colour in this figure legend, the reader is referred to the web version of this article.)

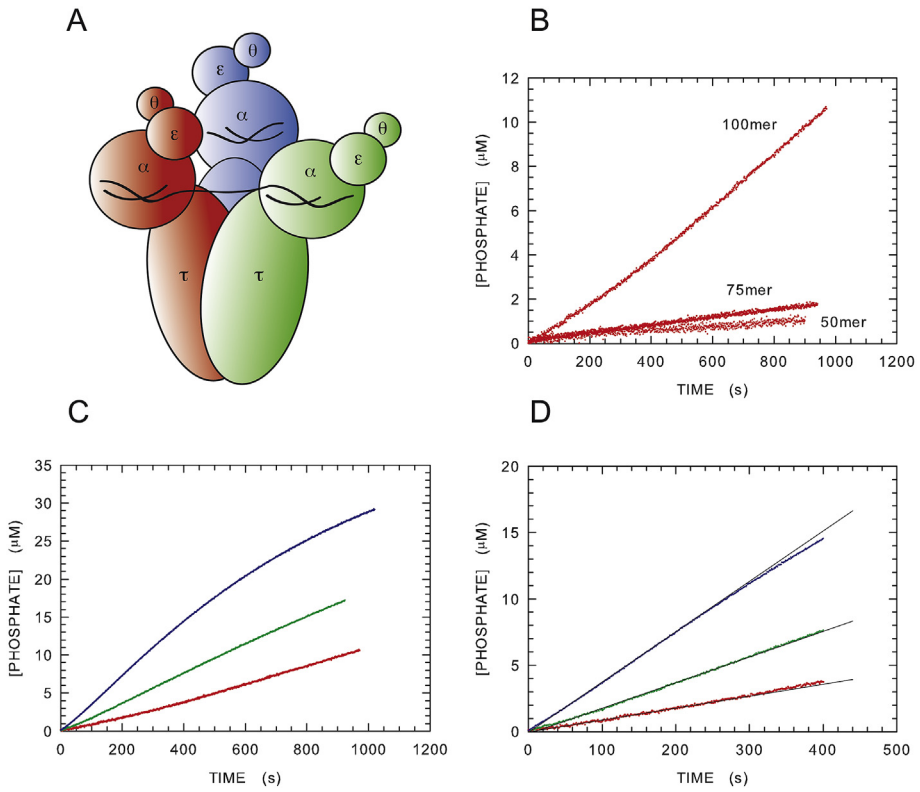

Fig. 3. Single-turnover assays of trimeric replicase. **A)** Cartoon of the $\tau_3\alpha_3\varepsilon_3\theta_3$ complex, represented with the same color code used for the DNA substrates (Fig. 2A). **B)** Single-turnover assays of DNA Polymerase activity of 200 nM $\tau_3\alpha_3\varepsilon_3\theta_3$ complex, in the presence of 100 μM dTTP, 200 nM 25mer DNA, and 200 nM of 100 mer, 75mer, or 50mer DNA. **C)** Single-turnover assays of DNA Polymerase activity of 200 nM $\tau_3\alpha_3\varepsilon_3\theta_3$ complex, in the presence of 25mer and 100mer DNA (200 nM each). Reaction mixtures contained dTTP (100 μM, red dots), dTTP and dATP (100 μM each, green dots), or dTTP, dATP and dGTP (100 μM each, blue dots). **D)** Detail of the reaction kinetics reported in Fig. 3C. Continuous lines represent the best fits used to calculate initial reaction velocities. (For interpretation of the references to colour in this figure legend, the reader is referred to the web version of this article.)

DNAs are considered, the template head was replicated: i) at the same initial velocity as the tail, in the presence of the 75mer or 100merDNA; ii) at a slower, if at all, initial velocity than the tail in the presence of the 50mer DNA, suggesting that a near downstream dsDNA inhibits elongation (Supplementary Figs 2–3).

We then performed single-turnover assays to test template head elongation, using the trimeric replicase (0.2 μM), a double-primed DNA and the 25mer DNA (0.2 μM each), in the presence of 100 μM dTTP. When the 50mer double-primed DNA was used, the extension of the template head was strongly inhibited (Fig. 3B), indicating that the dsDNA proximal to the tail hampers the elongation activity by a single α subunit of the $\tau_3\alpha_3\varepsilon_3\theta_3$ complex. A slightly higher activity was observed in the presence of the 75mer DNA (Fig. 3B), while the extension velocity of the 100mer DNA at the head site was significantly higher, and equal to 9 nM/s (Fig. 3B). Next, we performed further single-turnover assays using the trimeric replicase (0.2 μM), and both 100mer and 25mer DNA (0.2 μM each). When both dTTP and dATP were present (100 μM each), DNA Polymerase activity equalled 19 nM/s, indicating the concomitant extension of template head and tail (Fig. 3C and D). Finally, in the presence of dTTP, dATP, and dGTP (100 μM each), the extension rate increased further, being equal to 38 nM/s (Fig. 3C and D). This increase suggests that the activity at the expense of the 25mer DNA is equal to 19 nM/s, twice the activities observed with the double-primed DNA. However, it should be noted that the elongation rate of α subunit in the presence of the 25mer DNA is 5–6 times higher than the rate determined in the presence of the 100mer DNA (Supplementary Figs 2–3). Therefore, according to our observations, the activity of the two α subunits on the double-primed DNA slows down the extension of the single-primed DNA.

We demonstrated here that the trimeric replicase $\tau_3\alpha_3\varepsilon_3\theta_3$ is assembled *in vivo* by *E. coli* cells, and that this protein complex is competent in the simultaneous extension of three primers, asymetrically annealed to two DNA templates. Moreover, using double-primed DNAs as molecular rulers, we have shown that the parallel elongation by $\tau_3\alpha_3\varepsilon_3\theta_3$ of two primers annealed to the same DNA template depends on the interprimer distance, the minimum magnitude of which has to range between 40 and 65 nucleotides. These values correspond, when considering the average length of ssDNA [28], to about 260–420 Å. Taking into account the interaction between α subunits of the $\tau_3\alpha_3\varepsilon_3\theta_3$ complex (Supplementary Table 4), we propose a partial model of the trimeric replicase (Fig. 4, Supplementary Fig. 4, and animation provided online). With this model, we suggest that the replication of lagging strand is sustained by two α subunits, whose simultaneous elongation activity depends on a sufficiently long ssDNA connecting two active sites (Fig. 4). Upon shortening of this ssDNA to less than 40–65 nucleotides, further extension of the lagging strand could be exerted by a single α subunit, which, in turn, would pause its activity upon sensing a second dsDNA in close proximity (about 15 nucleotides, Fig. 3B). This temporary halt would trigger the switch of trimeric replicase to a new primer annealed to the lagging strand, starting the generation of a new Okazaki fragment. The trimeric replicase described here was

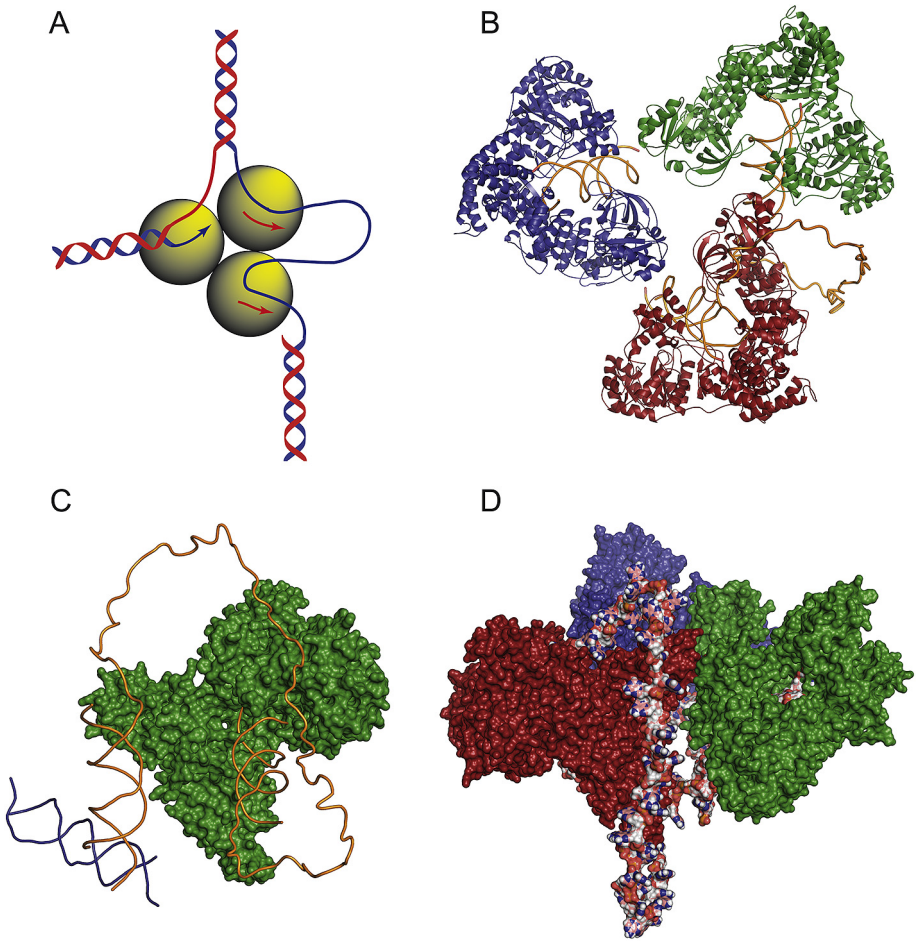

Fig. 4. Molecular model of trimeric replicase. **A)** Cartoon of 3 α subunits engaged in the simultaneous replication of leading (blue arrow) and lagging (red arrows) strands. **B)** Partial model of the trimeric replicase showing 3 α subunits associated with a single- and a double-primed DNA. The tertiary structure of full-lentgh *E. coli* α subunit was obtained from Swiss-Modeller [29], using as a template the *Thermus aquaticus* DnaE replicase (PDB 2hpm). The dsDNA structures are from *T. aquaticus* DnaE replicase (PDB 3e0d), and were positioned superimposing the *E. coli* protein model and the *T. aquaticus* polymerase in complex with DNA (PDB 3e0d). The ssDNA (65 nucleotides) was generated with Foldit [30]. The quaternary structure of the model was obtained imposing a distance between the K1037 of each subunit equal to 11.4 Å, which is the lentgh of the cross-linker used (BS3, Fig. 1E). **C)** Detail of the single- and the double-primed DNAs associated to the *E. coli* trimeric replicase. A single α subunit is shown in green. **D)** Side view of the molecular model reported in Fig. 4B. The structures were rendered with PyMol (The PyMOL Molecular Graphics System, version 1.3, Schrödinger, LLC). (For interpretation of the references to colour in this figure legend, the reader is referred to the web version of this article.)

obtained preventing the expression of γ subunit, which presence would imply the assembly of a dimeric enzyme. It will be interesting to ascertain the levels, *in vivo*, of τ and γ subunits as a function of the *E. coli* growth phase. It seems indeed reasonable to suppose that cells would benefit of trimeric replicase under conditions of active growth (and replication), while a dimeric replicase would suffice under stationary state or resting conditions.

Supplementary video related to this article can be found at http://dx.doi.org/10.1016/j.bbrc.2015.04.067.

Conflict of interest

None of the authors has any conflict of interest.

Acknowledgments

The authors are grateful to N. Maini and F. Francia for experimental assistance. A.M.S. was funded by the Royal Spanish College.

Appendix A. Supplementary data

Supplementary data related to this article can be found at http://dx.doi.org/10.1016/j.bbrc.2015.04.067.

Transparency document

Transparency document related to this article can be found online at http://dx.doi.org/10.1016/j.bbrc.2015.04.067.

References

[1] C.S. McHenry, DNA replicases from a bacterial perspective, Annu. Rev. Biochem. 80 (2011) 403–436.
[2] H. Maki, A. Kornberg, The polymerase subunit of DNA polymerase III of *Escherichia coli*, J. Biol. Chem. 260 (1985) 12987–12992.
[3] R.H. Scheuermann, H. Echols, A separate editing exonuclease for DNA replication: the ε subunit of *Escherichia coli* DNA polymerase III holoenzyme, Proc. Natl. Acad. Sci. U. S. A. 81 (1984) 7747–7751.
[4] S.A. Taft-Benz, R.M. Schaaper, The θ subunit of *Escherichia coli* DNA polymerase III: a role in stabilizing the ε proofreading subunit, J. Bacteriol. 186 (2004) 2774–2780.

[5] P.S. Studwell-Vaughan, M. O'Donnell, DNA polymerase III accessory proteins. V. θ encoded by *holE*, J. Biol. Chem. 268 (1993) 11785–11791.
[6] Z. Tsuchihashi, A. Kornberg, ATP interactions of the τ and γ subunits of DNA polymerase III holoenzyme of *Escherichia coli*, J. Biol. Chem. 264 (1989) 17790–17795.
[7] A.Y. Park, S. Jergic, A. Politis, et al., A single subunit directs the assembly of the *Escherichia coli* DNA sliding clamp loader, Structure 18 (2010) 285–292.
[8] D. Gao, C.S. McHenry, τ binds and organizes *Escherichia coli* replication proteins through distinct domains. Partial proteolysis of terminally tagged τ to determine candidate domains and to assign domain V as the α binding domain, J. Biol. Chem. 276 (2001) 4433–4440.
[9] A.L. Blinkowa, J.R. Walker, Programmed ribosomal frameshifting generates the *Escherichia coli* DNA polymerase III γ subunit from within the τ subunit reading frame, Nucleic Acids Res. 18 (1990) 1725–1729.
[10] H.G. Dallmann, R.L. Thimmig, C.S. McHenry, DnaX complex of *Escherichia coli* DNA polymerase III holoenzyme. Central role of τ in initiation complex assembly and in determining the functional asymmetry of holoenzyme, J. Biol. Chem. 270 (1995) 29555–29562.
[11] S. Maki, A. Kornberg, DNA polymerase III holoenzyme of *Escherichia coli*. III. Distinctive processive polymerases reconstituted from purified subunits, J. Biol. Chem. 263 (1988) 6561–6569.
[12] X.P. Kong, R. Onrust, M. O'Donnell, et al., Three-dimensional structure of the β subunit of *E. coli* DNA polymerase III holoenzyme: a sliding DNA clamp, Cell 69 (1992) 425–437.
[13] D.R. Kim, C.S. McHenry, Identification of the β-binding domain of the α subunit of *Escherichia coli* polymerase III holoenzyme, J. Biol. Chem. 271 (1996) 20699–20704.
[14] P. McInerney, A. Johnson, F. Katz, et al., Characterization of a triple DNA polymerase replisome, Mol. Cell. 27 (2007) 527–538.
[15] N.A. Tanner, G. Tolun, J.J. Loparo, et al., *E. coli* DNA replication in the absence of free β clamps, EMBO J. 30 (2011) 1830–1840.
[16] R.E. Georgescu, I. Kurth, M.E. O'Donnell, Single-molecule studies reveal the function of a third polymerase in the replisome, Nat. Struct. Mol. Biol. 19 (2012) 113–116.
[17] R.E. Georgescu, N. Yao, C. Indiani, et al., Replisome mechanics: lagging strand events that influence speed and processivity, Nucleic Acids Res. 42 (2014) 6497–6510.
[18] D. Bressanin, A. Stefan, F. Dal Piaz, et al., Proteolysis of the proofreading subunit controls the assembly of *Escherichia coli* DNA polymerase III catalytic core, Biochim. Biophys. Acta 1794 (2009) 1606–1615.
[19] E. Conte, G. Landolfi, G. Vincelli, et al., pGOODs: new plasmids for the co-expression of proteins in *Escherichia coli*, Biotechnol. Lett. 33 (2011) 1815–1821.
[20] M.A. Bradford, A rapid and sensitive method for the quantitation of microgram quantities of protein utilizing the principle of protein-dye binding, Anal. Biochem. 72 (1976) 248–254.
[21] E. Conte, G. Vincelli, R.M. Schaaper, et al., Stabilization of the *Escherichia coli* DNA polymerase III ε subunit by the θ subunit favors *in vivo* assembly of the Pol III catalytic core, Arch. Biochem. Biophys. 523 (2012) 135–143.
[22] M.C. Monti, S.X. Cohen, A. Fish, et al., Native mass spectrometry provides direct evidence for DNA mismatch-induced regulation of asymmetric nucleotide binding in mismatch repair protein MutS, Nucleic Acids Res. 39 (2011) 8052–8064.
[23] A.S. Guillén Suárez, A. Stefan, S. Lemma, et al., Continuous enzyme-coupled assay of phosphate- or pyrophosphate-releasing enzymes, Biotechniques 53 (2012) 99–103.
[24] S. Hamdan, E.M. Bulloch, P.R. Thompson, et al., Hydrolysis of the 5′-*p*-nitrophenyl ester of TMP by the proofreading exonuclease (ε) subunit of *Escherichia coli* DNA polymerase III, Biochemistry 41 (2002) 5266–5275.
[25] S.A. Taft-Benz, R.M. Schaaper, The C-terminal domain of DnaQ contains the polymerase binding site, J. Bacteriol. 181 (1999) 2693–2695.
[26] E.F. DeRose, T. Darden, S. Harvey, et al., Elucidation of the ε-θ subunit interface of *Escherichia coli* DNA polyerase III by NMR spectroscopy, Biochemistry 42 (2003) 3635–3644.
[27] M.H. Lamers, R.E. Georgescu, S. Lee, et al., Crystal structure of the catalytic α subunit of *E. coli* replicative DNA polymerase III, Cell 126 (2006) 881–892.
[28] M.C. Murphy, I. Rasnik, W. Cheng, et al., Probing single-stranded DNA conformational flexibility using fluorescence spectroscopy, Biophys. J. 86 (2004) 2530–2537.
[29] K. Arnold, L. Bordoli, J. Kopp, et al., The Swiss-Model workspace: a web-based environment for protein structure homology modelling, Bioinformatics 22 (2006) 195–201.
[30] S. Cooper, F. Khatib, A. Treuille, et al., Predicting protein structures with a multiplayer online game, Nature 466 (2010) 756–760.